



Contents lists available at ScienceDirect

## Journal of Orthopaedic Translation

journal homepage: [www.journals.elsevier.com/journal-of-orthopaedic-translation](http://www.journals.elsevier.com/journal-of-orthopaedic-translation)

## Rotator cuff healing is regulated by the lymphatic vasculature

Xiaopeng Tong<sup>a,b,c</sup>, Tao Zhang<sup>a,b,c</sup>, Shengcan Li<sup>a,b,c</sup>, Yang Chen<sup>a,b,c</sup>, Yan Xu<sup>a,b,c</sup>,  
Chao Deng<sup>b,c,d</sup>, Jianzhong Hu<sup>b,c,d,\*\*</sup>, Hongbin Lu<sup>a,b,c,\*</sup><sup>a</sup> Department of Sports Medicine, Xiangya Hospital, Central South University, Changsha, 410008, China<sup>b</sup> Key Laboratory of Organ Injury, Aging and Regenerative Medicine of Hunan Province, Changsha, 410008, China<sup>c</sup> National Clinical Research Center for Geriatric Disorders, Xiangya Hospital, Central South University, Changsha, 410008, China<sup>d</sup> Department of Spine Surgery and Orthopaedics, Xiangya Hospital, Central South University, Changsha, 410008, China

## ARTICLE INFO

## Keywords:

Lymphatic vessel  
Lymphatic drainage  
Rotator cuff healing  
Bone-tendon interface  
Lymphatic vessel inhibitor

## ABSTRACT

**Background:** Despite great advances in surgical techniques for rotator cuff tear (RCT) over the past decades, the postoperative failure rate of RCT is still high due to the poor healing competence of bone-tendon interface (BTI). The lymphatic vasculature plays a regulatory role in inflammatory disease and affects tissue healing. However, whether lymphangiogenesis and the role of lymphatic vasculature in the physiopathological process of rotator cuff (RC) injury remains unknown.

**Methods:** In this study, we constructed a mouse RC injury model and the BTI samples were collected for measurement. Firstly, immunofluorescence was used to investigate the temporal and spatial distribution of lymphangiogenesis in BTI area at different post-injury time points. Subsequently, the mice of experimental group were gavaged with the lymphatic inhibitors (SAR131675) on the first postoperative day to inhibit lymphangiogenesis, while the control group was treated with the vehicle. At postoperative week 2 and 4, the samples were collected for immunofluorescence staining to evaluate lymphatic angiogenesis inhibition. At postoperative week 4 and 8, The supraspinatus (SS) tendon–humeral complexes were collected for bone morphometric, histological and biomechanical tests to assess the healing outcome of the BTI.

**Results:** Immunofluorescence results showed that the lymphatic proliferation in the BTI injury area and increased in consistence with the healing time, and the lymphatic hyperplasia area significantly diminished at postoperative week 4. The lymphatic hyperplasia area in the SAR group was significantly lower than that in the control group both at 2 and 4 weeks postoperatively. Moreover, the administration of SAR131675 significantly impeded RC healing, as evidenced by lower histological scores, lower bone morphometric parameters, and worse biomechanical properties in comparison with that in control group at postoperative weeks 4 and 8.

**Conclusion:** Lymphangiogenesis plays a positive role in RC healing, and targeting the lymphatic drainage at healing site may be a new therapeutic approach to promote RC injury repair.

**The translational potential of this article:** This is the first study to assess the specific role of lymphatic vessels in RC healing, and improving lymphatic drainage may be a potential new therapeutic approach to facilitate repair of BTI. Further, our study provides a reference for possible future treatment of BTI by intervening the lymphatic system.

## Introduction

Rotator cuff tear (RCT) is a very common shoulder injury that usually results in shoulder pain and joint weakness. For patients with RCT that fail conservative treatment, surgery is usually required to achieve anatomical restoration between bone and tendon [1,2]. Previous studies have shown that the recurrence rates of RCT are as high as 20–94%

[3–5]. The main difficulty of rotator cuff (RC) injury healing is that the original attachment structural between tendon and bone cannot be regenerated after injury. Histologically, the attachment structural termed bone-tendon interface (BTI) classically consists of four layers: bone, calcified fibrocartilage, uncalcified fibrocartilage, and tendon [6–8]. The main function of BTI is to effectively disperse stress and facilitate mechanical load conduction. Due to its poor blood supply and the weak

\* Corresponding author. Xiangya Hospital, No. 87, Xiangya Road, Kaifu District, Changsha, 410008, China.

\*\* Corresponding author. Xiangya Hospital, No. 87, Xiangya Road, Kaifu District, Changsha 410008, China.

E-mail addresses: [jianzhonghu@hotmail.com](mailto:jianzhonghu@hotmail.com) (J. Hu), [hongbinlu@hotmail.com](mailto:hongbinlu@hotmail.com) (H. Lu).<https://doi.org/10.1016/j.jot.2022.09.014>

Received 25 September 2022; Accepted 28 September 2022

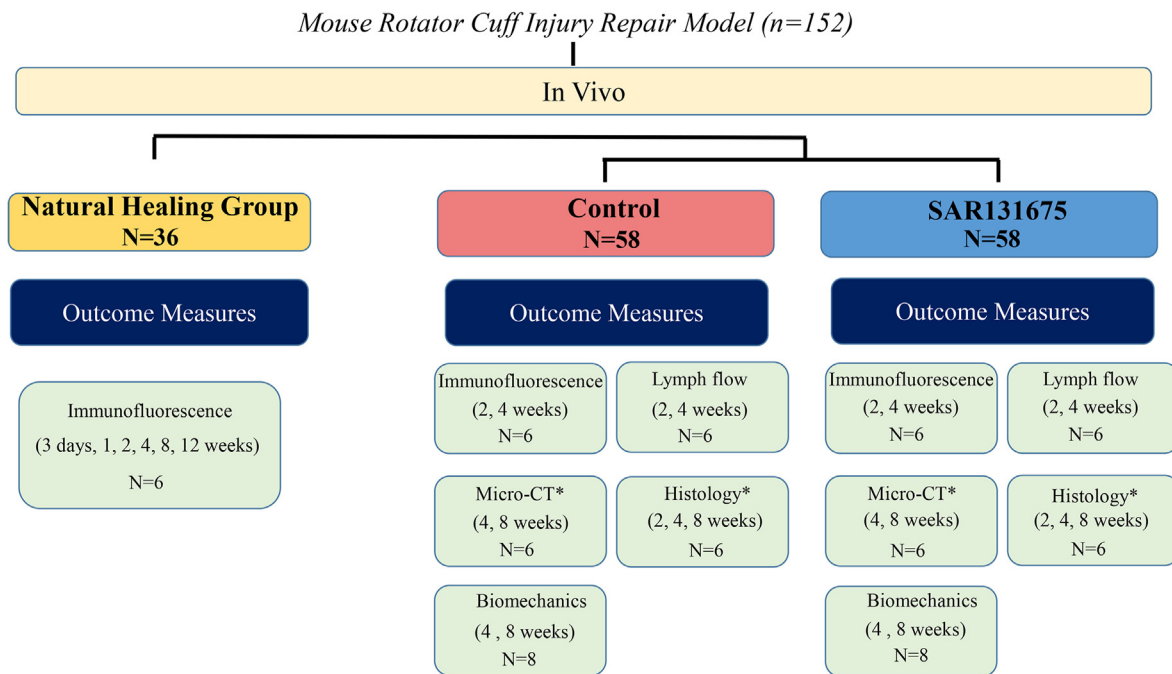


**Figure 1.** Study design flowchart. \* indicates the same samples at 4 and 8 weeks after repair surgery for micro-CT and histological evaluation.

regeneration ability, it is difficult to quickly restore the normal gradient hierarchy and mechanical properties [1,9]. Acute RC injury usually results in high levels of inflammation and recruitment of immune cells that secrete many factors that influence the healing response and promote scar formation [10]. During the healing of the fibrocartilage layer at RC insertion site, the regeneration undergoes local necrotic tissue degradation, collagen fiber rearrangement and fibrochondrocyte maturation during the remodeling phase, and the infiltration of inflammatory mediators across the entire healing process [11,12]. Therefore, it is urgent to find out the factors affecting the enthesis repair in the physiopathological process of RCT healing.

The lymphatic system plays an important role in maintaining both metabolic and tissue fluid homeostasis, the primary function of lymphatic vessels is to transport tissue fluid, exudate plasma proteins, and cells from body tissues back to the circulatory system [13]. The important role of lymphangiogenesis in tissue regeneration and remodeling has been widely documented in enteritis, acute or chronic arthritis, and myocardial infarction [14–17]. A common feature among these diseases is tissue edema and inflammation, which increases the need for fluid removal and immune cell transportation [13]. When the lymphatic network is remodeled, with the increase of tissue excretion capacity, it may be beneficial to tissue repair by enhancing the clearance of accumulated tissue fluid, immune cells, tissue fragments, chemokines, growth factors, etc [18]. Studies have found that the inhibition of post-injury lymphatic vessel growth exacerbates joint synovitis and causes bone erosion and cartilage loss [16,19]. However, whether lymphangiogenesis occurs during RCT repair and its effect on BTI healing remains further investigation.

VEGF-C and VEGF-D are major growth factors in inflammatory lymphangiogenesis, and they are primarily transmitted through VEGFR-3 receptors on lymphatic endothelial cells [20]. Taken together, VEGF-C/VEGF-D-VEGFR-3 axis constitutes a signaling system for lymphatic endothelial cell growth, migration, and survival [13,20]. Therefore, inhibiting the activation of VEGFR-3 can effectively restrain the autophosphorylation of VEGFR-3, which in turn suppress the lymphangiogenesis process [21]. SAR131675 (SAR) is a VEGFR-3 inhibitor that is 50 and 10 times more selective for VEGFR-3 than for VEGFR-1/2 [22]. Previous studies have shown that SAR can effectively inhibit

lymphangiogenesis in models of bronchitis and diabetic nephropathy [22,23]. The role of lymphatic system in RC injury healing has not been reported.

We hypothesized that lymphangiogenesis plays a positive role in RCT healing, and inhibition of lymphangiogenesis would impair the healing outcome after RC injury. In this study, we first established a mouse RC insertion injury model to verify the spatial and temporal distribution of lymphatic vessels in the injured area. We then examined the inhibition of VEGFR-3 inhibitor (SAR131675) on lymphangiogenesis in the injured area and determined its effect on supraspinatus tendon drainage. Further, we assessed the role of lymphangiogenesis in RC injury healing.

## Materials and methods

All the animal tests were approved by the Animal Ethics Committee of Xiangya Hospital, Central South University (No. 201703222), and in accordance with guidelines for reporting in vivo experiments in animal studies [24].

### Study design

In this study, a total of 152 male C57BL/6 mice (8-weeks-old, male, 22–24 g) underwent an acute RC injury repair surgery (Fig. 1). To explore the temporal and spatial distribution trend of lymphangiogenesis in the BTI injury area, 36 samples were collected for immunofluorescence staining at 3 d, 1, 2, 4, 8 and 12 weeks postoperatively. Subsequently, the remaining mice that underwent surgery were randomly divided into control group and experimental group. The experimental group was given SAR by intragastric administration on the first day after surgery, while the control group was given the vehicle by intragastric administration. At postoperative week 2 and 4 weeks, supraspinatus tendon (SST) entheses were collected for lymphatic immunofluorescence staining to evaluate lymphatic angiogenesis and 24 mice were used to assess changes in the drainage capacity of the SST. The SS-humeral complexes were collected at postoperative week 4 and 8 for micro-computed tomography (micro-CT), histological and biomechanical tests to assess the healing quality of BTI.

### Rotator cuff injury repair model

The C57BL/6 mice underwent left RC repair surgery as reported in previous studies [25,26]. After the mice were anesthetized with 0.3% pentobarbital (0.6 ml/20 g; Sigma–Aldrich, St. Louis, MO), a longitudinal incision was made on the skin surface of the left shoulder. The deltoid was incised and the muscle was pulled apart to fully expose the RC insertion. A 6–0 PDS line (No. 6–0, Ethicon, NJ, USA) was inserted into the SST and quickly separated from the insertion of the greater tubercle of the humerus with an 11 blade. Subsequently, the fibrocartilage and part of the subchondral bone at the insertion point were removed by curettage, and a 30G needle was used to create a bone tunnel laterally through the proximal humerus. The PDS wire was passed through the bone tunnel to fix the SST tissue at the original implantation site. After confirming that there was no active bleeding at the surgical site, the deltoid muscle and skin were sutured layer by layer. Postoperatively, penicillin G was administered once a day for three days to prevent infection.

### Drug administration

The VEGFR-3 inhibitor SAR131675 (Selleck Chemicals, Munich, Germany) was dissolved in 0.5% sodium carboxymethylcellulose (CMC-Na) solution according to the producer's instructions. Mice in the experimental group were gavaged with SAR (50 mg/kg/day) on the first postoperative day, once a day, until 2 weeks, 4 weeks or 8 weeks after surgery. The control group was gavaged with 0.5% CMC-Na.

### Immunofluorescence staining

After the mice were euthanized, the samples were fixed in 4% paraformaldehyde overnight, and the residual paraformaldehyde was cleaned with PBS for decalcification and gradient dehydration. Afterward, the samples were embedded using the tissue-tek® O.C.T. Compound (SAKURA, Torrance, USA) and cut into 8 µm thick sagittal sections on a frozen micrograph machine. For immunofluorescence staining, tissue sections were rewarmed at room temperature for 30min and then blocked with 5% bovine serum albumin for 1 h to block non-specific antigen expression. After the corresponding antigen was incubated overnight with anti-LYVE-1 (AngioBio, 11–034), anti-VEGFR-3 antibody (RD, AF743), anti-Ki-67 antibody (abcam, ab16667) at 4°, frozen section samples were washed three times with PBS to remove residual primary antibody. The corresponding secondary antibody Alexa Fluor 488 (Abcam, Ab159153), Alexa-Fluor 594 (Abcam, ab150132), and Alexa-Fluor 647 (Abcam, ab150075) were incubated with samples at room temperature for 1 h, then washed three times with PBS and restained with DAPI. Images were observed using a Zeiss AxioImager. M2 microscope (Zeiss, Solms, Germany) equipped with an Apotome.2 System. The positive area of LYVE-1 and VEGFR-3 was measured by defining the region of interest (ROI) at the insertion injury. The positive staining area (%) was calculated by dividing the positive staining area by the total ROI area using Image-Pro Plus software (version 6.0.0; Media Control Netics Inc).

### Lymph flow assessment using Evans blue dye

Evans blue dye (Sigma Aldrich) was dissolved in PBS to prepare a 1% dye solution. At 2 and 4 weeks after surgery, 0.3 µL was injected into the SST of mice in the control group and the experimental group using a Hamilton syringe. After 24 h, the mice were sacrificed and Evans blue dye was extracted from SST and incubated in formamide (Sigma–Aldrich) at 55 °C for 5.5 h. The background-subtracted absorbance was measured with a microplate reader (Varioskan LUX, Thermo, USA) by measuring at 620 nm. The concentration of dye in the extracts was calculated from a standard curve of Evans blue in formamide and was presented as absolute amount of dye that remained in the SST.

### Micro-CT scanning

Before micro-CT Scanning, the SST-humerus complexes were fixed in 4% paraformaldehyde for 24 h, washed with running water, and then soaked in PBS for detection. Afterward, the specimens were scanned using micro-CT (vivaCT 80, Scanco Medical, Switzerland). The specific parameters of the scan were as follows: voltage 55 KV, current 145 µA, resolution 11.4 µm per pixel. Raw images were 3D reconstructed and visualized using Amira software (Thermo Scientific, Waltham, MA). The region of interest included trabecular bone within the humeral head near the tendon attachment (within approximately 1 mm) and proximal to the growth plate. The data analysis software (CT Analyzer v1.11, Bruker Corporation, Germany) was used to calculate bone volume fraction (BV/TV), trabecular thickness (Tb.Th), trabecular number (Tb.N) and trabecular separation (Tb.Sp). The data was evaluated in a blinded manner.

### Histological evaluation

After micro-CT scanning, the specimens were decalcified with 10% EDTA solution. The samples were dehydrated in a gradient manner, embedded in paraffin, and sectioned (sagittal incision of humeral head and SST) to 5 µm. Representative sections were stained with hematoxylin and eosin (H&E) or fast green-toluidine blue (FG&TB) (Sigma–Aldrich, St. Louis, MO). Tissue sections were observed using a light microscope (CX31, Olympus, Germany). Healing of the RC insertion was assessed by two blinded observers according to a previously reported bone-tendon healing scoring system [26], which includes: cellularity, vascularity, continuity, fibrocartilage cells, tidemark and ranked on a scale from 1 to 4 (Table S1) [26]. A higher histology score indicates improved or more mature tendon-to-bone healing.

### Biomechanical testing

A biomechanical testing system (model 5942, Instron, MA) was used to detect the failure load, ultimate stress, stiffness and distance of the repair enthesis. Briefly, after removing the sutures for repair of the RC insertion injury, the SST was secured in the upper clamp using sandpaper, while the humeral shaft was fixed in the lower clamp. Before testing, the width and thickness of the SST were measured with a caliper under the same tensile load (0.1 N), then the cross-sectional area (CSA) was calculated. During the formal test, the samples in the fixture were preloaded under the condition of 0.1 N and loaded at a rate of 0.03 mm/s to failure. All experiments were carried out at room temperature, and 0.9% saline was used to keep the samples fresh during the test.

### Statistical analysis

Statistical analyses were performed using SPSS 25.0 software (SPSS, USA). All quantitative data were expressed as mean ± standard deviation (SD). Data were confirmed normal distribution by Shapiro–Wilk test and homoscedasticity by Levene's Test before t-test analysis. Unpaired two-tailed Student's t-test was used to determine statistical significance between two groups, while the histological scores was performed using the Mann–Whitney test.  $P < 0.05$  was considered statistically significant.

## Results

### Spatiotemporal expression of lymphatic vessels

Immunofluorescence staining of lymphatic vessels specific markers LYVE-1 and VEGFR-3 revealed lymphatic vessels surrounding the uninjured RC, but only LYVE-1 marker was observed (Fig. S1). This suggests that the lymphatic drainage exists surrounding SST enthesis when in its normal status. At postoperative week 2, lymphatic proliferation significantly increased at the tendon tip of injury area and increased with repair



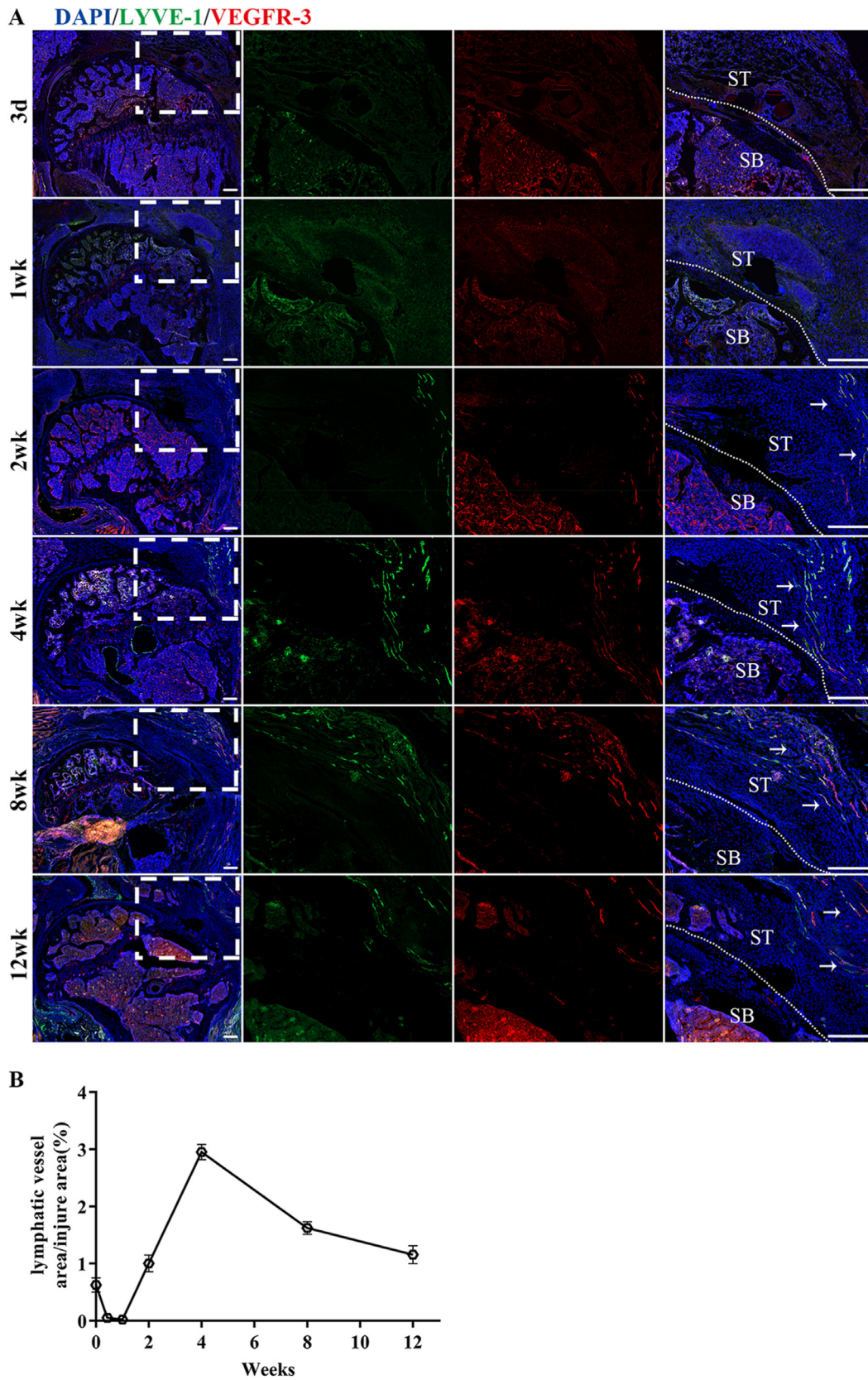


**Figure 2.** The spatial and temporal distribution characteristics of lymphatic vessels in the injured area after RC injury (A) Representative immunofluorescence images of lymphatic vessels (LYVE-1 and VEGFR-3 co-staining) at different times after RC injury-repair. The area selected by the rectangle dashed line is the local magnified area. The dashed line denotes repaired insertion of the examples. The white arrow indicates proliferating lymphatic vessels. SB, subchondral bone; ST, supraspinatus tendon; Scale bars = 400  $\mu$ m. (B) Quantitative analysis of lymphatic vessels' positive staining areas at different times after RC injury-repair. n = 6 for each group. \* $P < 0.05$ .



time. Four weeks after surgery, the lymphangiogenesis area gradually decreased. At postoperative week 12, the lymphatic hyperplasia area was greatly reduced. The process of repair of RC insertion healing was followed by the proliferation and remodeling of lymphatic vessels, indicating that lymphangiogenesis in the area of insertion injury might be involved in the repair process of RC injury (Fig. 2).

*Assessment of lymphatic endothelial cell proliferation*

As shown in Fig. S2, proliferating lymphatic endothelial cell nuclei were observed at both 2 and 4 weeks postoperatively. At postoperative week 2, the proliferation of lymphatic endothelial cells in the injured area was significantly increased, while at postoperative week 4, the proliferation of lymphatic endothelial cells was significantly decreased.

These results indicated that the lymphatic endothelial cells in the injured area had the ability to proliferate, and the proliferation decreased with the change of repair time.

*Analysis of the inhibition of lymphangiogenesis using SAR131675*

Immunofluorescence results showed that lymphatic hyperplasia area in SAR groups were significantly lower than that in the control groups at postoperative week 2 and 4 ( $P < 0.05$ ) (Fig. 3). The experimental data indicated that SAR could effectively inhibit the formation of lymphatic vessels in the injured area after RC injury. These results provided support for us to further explore the influence of lymphangiogenesis inhibition on the repair of tendon insertion injury.

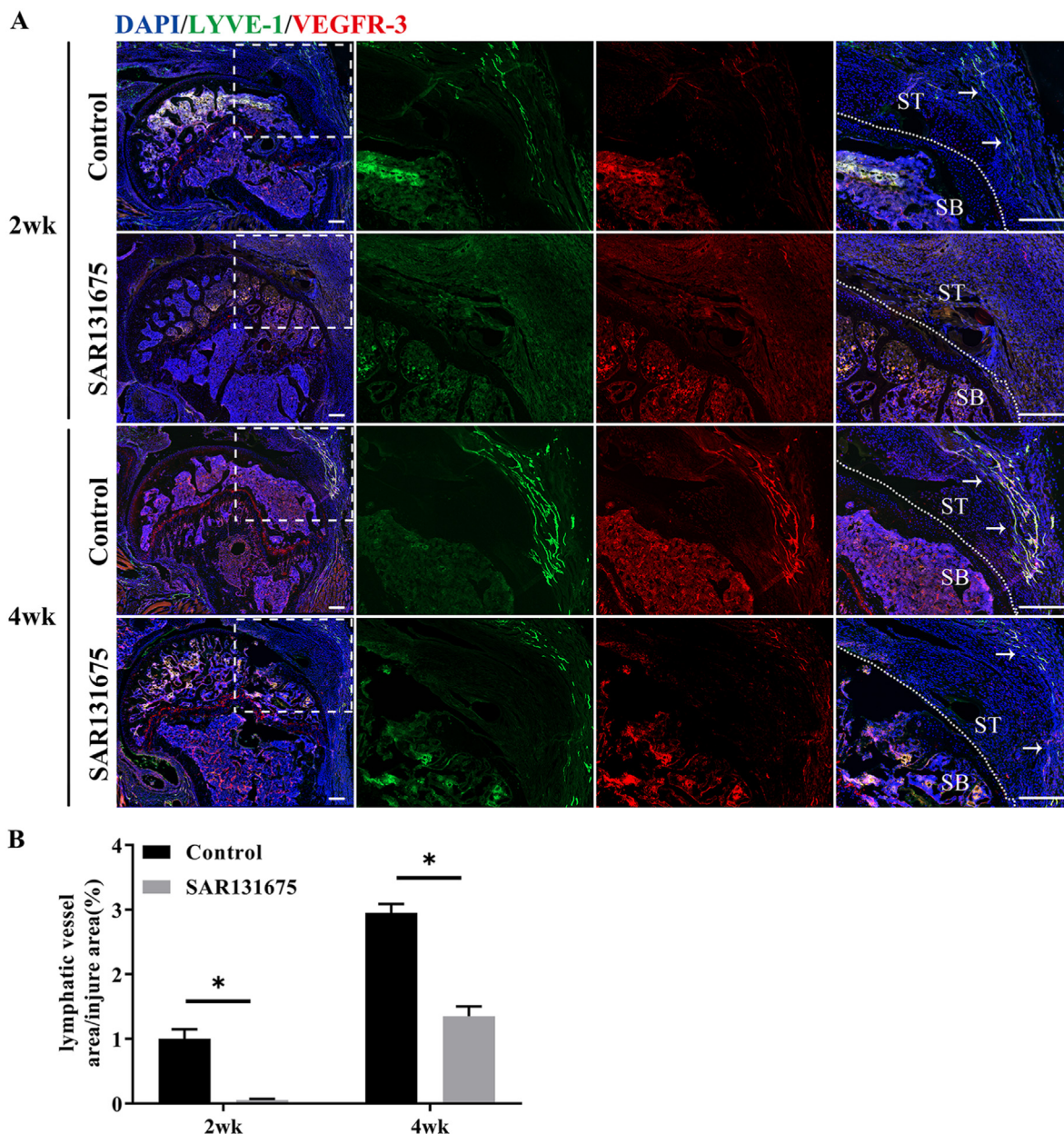


**Figure 3.** SAR131675 effectively inhibits the formation of lymphatic vessels in the injured area after RC injury (A) Representative immunofluorescence images of lymphatic vessels (LYVE-1 and VEGFR-3 co-staining) at the control and SAR131675 groups postoperatively 2 and 4 weeks. The area selected by the rectangle dashed line is the local magnified area. The dashed line denotes repaired insertion of the examples. The white arrow indicates proliferating lymphatic vessels. SB, subchondral bone; ST, supraspinatus tendon; Scale bar = 400 μm. (B) Quantitative analysis of lymphatic vessels positive staining areas at the healing area. n = 6 for each group. \* $P < 0.05$ .

Blocking lymphangiogenesis led to decreased lymph flow

Next, we investigated whether blocking lymphangiogenesis at the site of insertion injury might lead to a decrease in the lymphatic drainage capacity of the tendon (Fig. 4). For this, we injected Evans blue dye into the supraspinatus tendons of control or SAR mice. Evans blue was extracted from mouse tendons 24 h after tendon injection by Evans blue uptake by lymphatic vessels. It was found that the content of Evans blue in the tendons of the SAR group was significantly higher than that of the control group ( $P < 0.05$ ), indicating that the function of lymphatic clearance was weakened.

Micro-CT analysis

The bone repair of the insertion site after RC injury was evaluated by 3D reconstruction images and quantitative analysis of bone morphological parameters (Fig. 5). Compared with the uninjured normal group, both groups (control and SAR) had significant bone loss at 4 weeks postoperatively, with partial recovery at 8 weeks postoperatively. Quantitatively, BV/TV, Tb.N were significantly higher in the control group than in the SAR group at 4 and 8 weeks after surgery ( $P < 0.05$ ). In terms of Tb.Th, 4 weeks after surgery, the SAR group was significantly lower than the control group ( $P < 0.05$ ), but at 8 weeks after surgery, the difference was not statistically significant. At the same time, the Tb.Sp of the repaired bone at the insertion point in the SAR group was significantly increased compared with the control group ( $P < 0.05$ ), indicating a worse quality of bone healing. These results revealed that inhibiting the proliferation of lymphatic vessels in the injured area of the insertion will hinder the bone repair of the insertion after injury.

Histological analysis

H&E and FG&TB staining showed that the interstitial structural repair was gradually improved with the extension of repair time (Figs. 6 and 7). Eosinophils and extensive lymphocyte infiltration were observed in both groups 2 weeks after surgery, and inflammatory cell infiltration was more obvious in the SAR group than in the control group. Four weeks after surgery, compared with the control group, the tissue structure of SAR tendon–bone junction was loose with obvious fractures. At 8 weeks postoperatively, the control group had more mature tendon-bone

attachment than the SAR group. The fibrocartilage area in the control group was significantly larger than that in the SAR group (Figs. 7 and 8B). The results of semi-quantitative analysis using the improved bone-tendon healing scale showed that the tendon-bone maturity score of both groups increased with the extension of healing time. There was no difference in maturity score at week 2 after surgery between the two groups. At 4 and 8 weeks postoperatively, the scores of the control group were significantly higher than those of the SAR group (Fig. 8C).

Biomechanical testing

In the biomechanical testing (Fig. S3), all specimens ruptured at the RC enthesis. The effects of lymphatic inhibitors on the biomechanics of tendon-bone healing were observed at 4 and 8 weeks after repair surgery (Fig. 9). Three parameters of failure load, stiffness and ultimate strength were tested. At 4 and 8 weeks after surgery, the failure load and ultimate strength of the SAR group were significantly lower than those of the control group ( $P < 0.05$ ). In terms of stiffness, 4 weeks after surgery, the SAR group was significantly lower than the control group ( $P < 0.05$ ), but at 8 weeks after surgery, the difference was not statistically significant. These results indicated that inhibition of lymphatic proliferation in the enthesis injury area may hinder the improvement of biomechanical properties after insertion injury.

Discussion

In this study, we found for the first time that there existed lymphatic proliferation and remodeling at the injury area after RC injury, which involved in the repair process. We also verified the proliferation capacity of lymphatic endothelial cells in the injured area. Furtherly, our results showed that inhibiting the lymphatic proliferation in the RC healing period significantly reduced the tendon lymphatic drainage capacity, as well as impaired BTI healing capacity, which was evidenced by decreased bone healing parameters, histological scores, and biomechanical properties in the lymphatic inhibitor group. The results show that the ingrowth of lymphatic vessels in the injured BTI area is indispensable for RC healing.

Previous studies have found the RC healing process goes through inflammatory, proliferative and remodeling phases [11,27], and lymphangiogenesis plays positive roles in inflammation mediation, wound

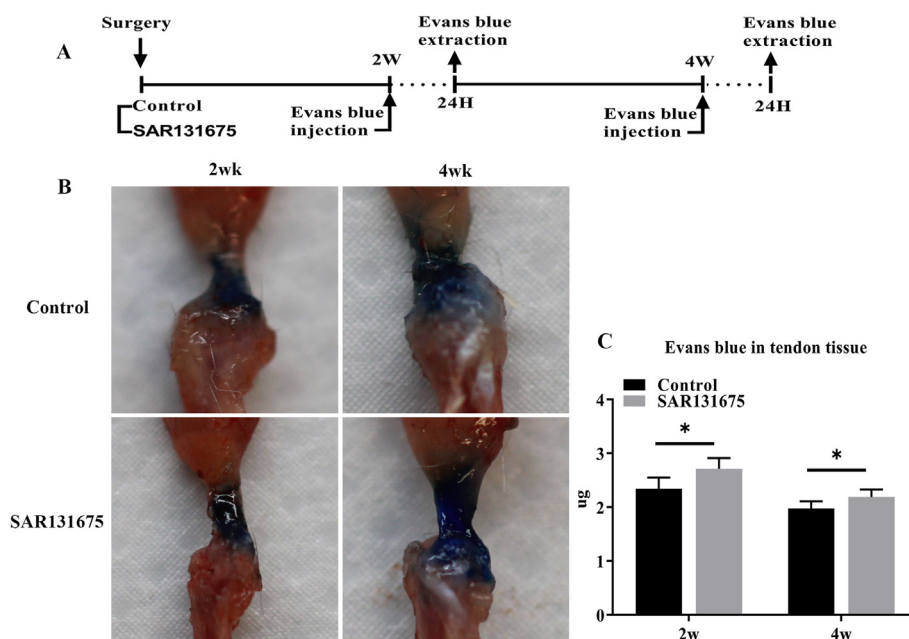
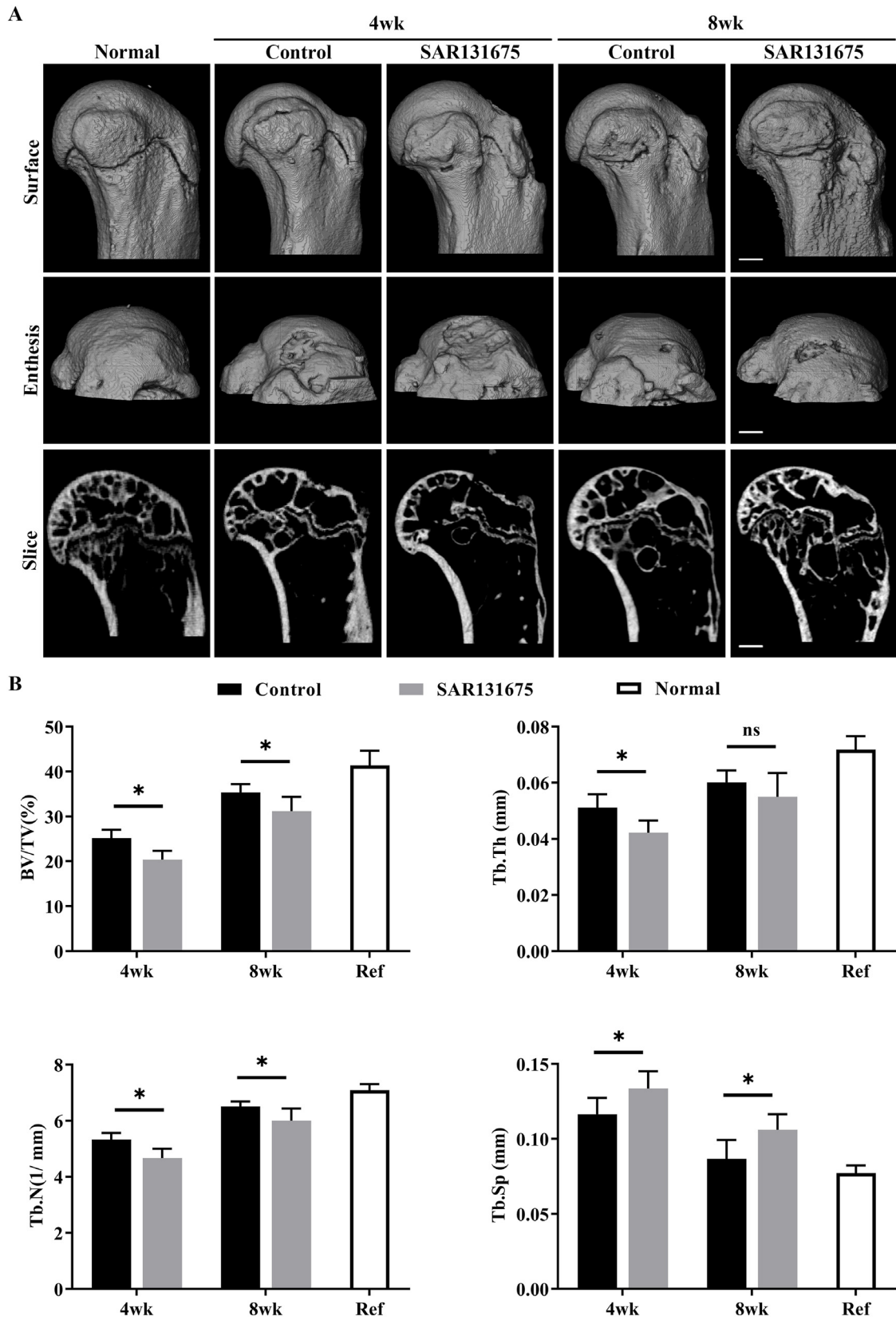
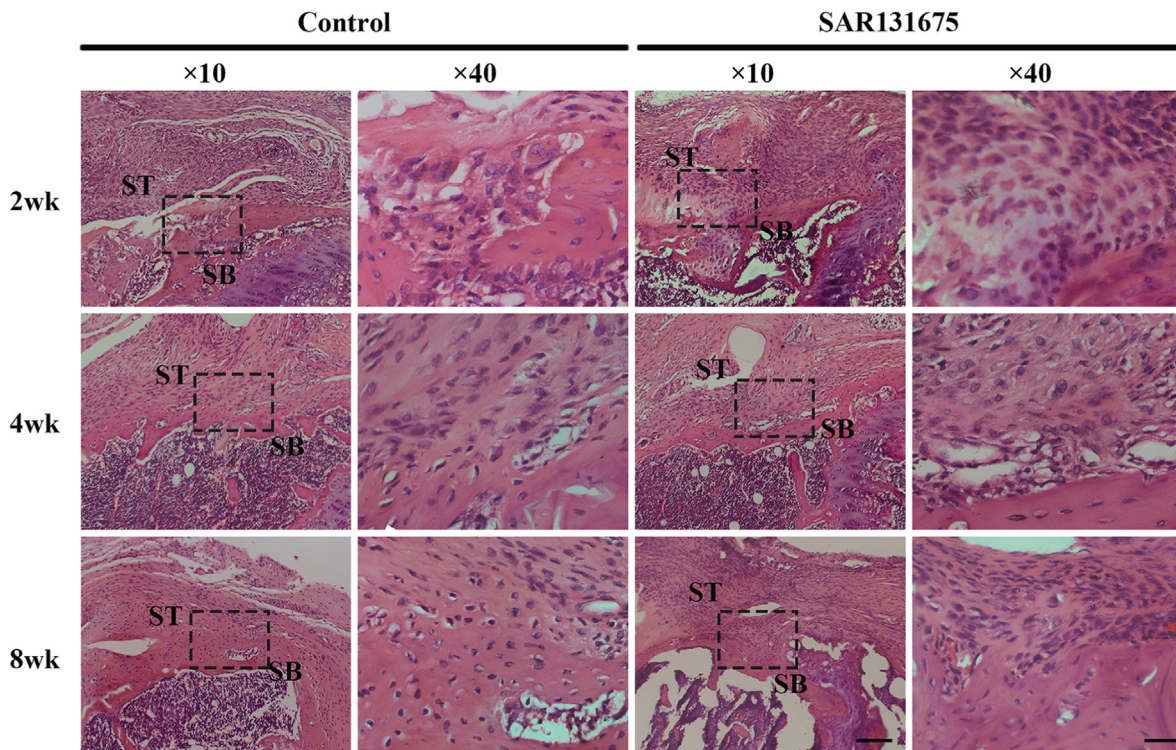


Figure 4. Inhibition of lymphangiogenesis at the site of injury results in a decrease in the ability of tendon lymphatic drainage (A) Evans blue dye was intradermally injected into the SS tendon of mice in the control group and the experimental group and was extracted 24 h after the dye injection at postoperative week 2 and 4. (B) Representative pictures before Evans blue extraction. (C) The total dye remaining in the SS tendon. n = 6 for each group. \* $P < 0.05$ . (For interpretation of the references to colour in this figure legend, the reader is referred to the Web version of this article.)



**Figure 5.** Inhibition of lymphangiogenesis at the site of injury reduces bone morphometric parameters (A) Representative micro-CT three-dimensional reconstruction images and sagittal sections reconstruction images of the RC healing site for all groups at postoperative week 4 and 8, Scale bar = 600  $\mu$ m. (B) The morphological parameters of subchondral bone in the control and SAR131675 groups. BV/TV, bone volume fraction; Tb.Th, trabecular thickness; Tb.N, trabecular number; Tb.Sp, trabecular separation. n = 6 for each group. \**P* < 0.05.





**Figure 6.** Evaluation of insertion healing using hematoxylin and eosin (H&E) staining. Representative H&E images of BTI at 2, 4 and 8 weeks postoperatively for all groups. The area selected by the rectangle dashed line is the local magnified area. SB, subchondral bone; ST, supraspinatus tendon; Scale bars indicate 200 μm for the overall picture and 50 μm for the local magnified area.

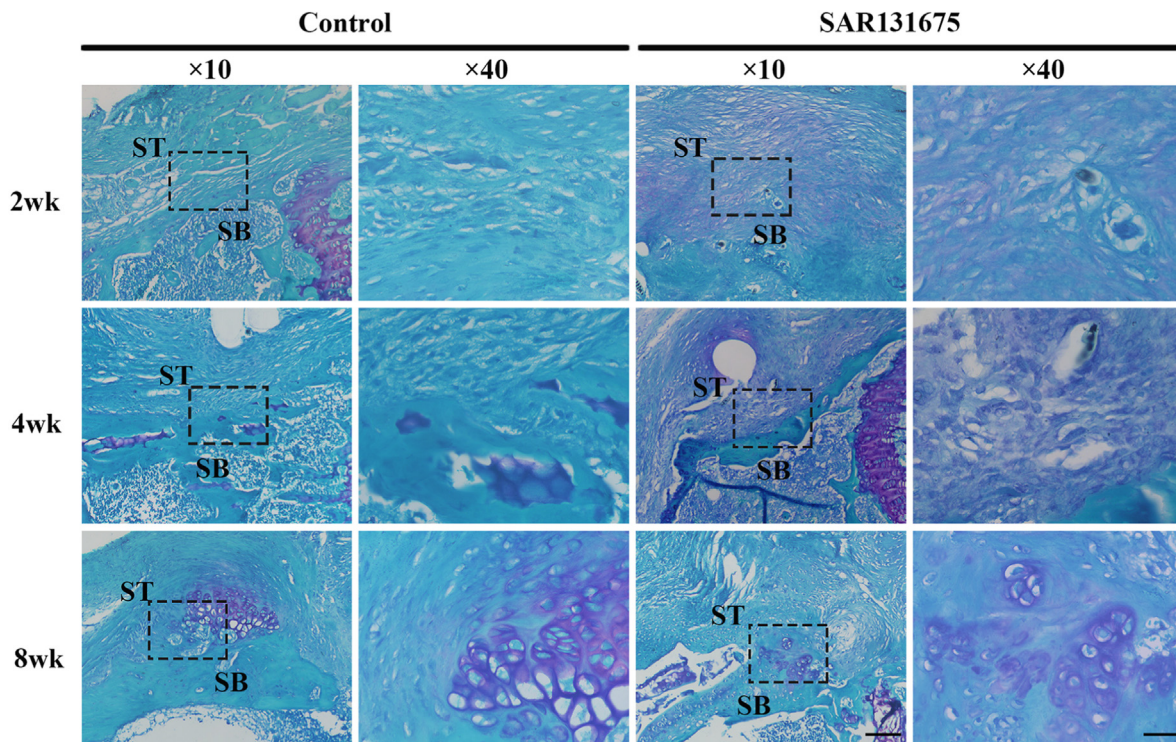


**Figure 7.** Evaluation of fibrocartilage formation at the insertion using fast green-toluidine blue (FG&TB) staining. Representative FG&TB images of BTI at 2, 4 and 8 weeks postoperatively for all groups. The area selected by the rectangle dashed line is the local magnified area. SB, subchondral bone; ST, supraspinatus tendon; Scale bars indicate 200 μm for the overall picture and 50 μm for the local magnified area. (For interpretation of the references to colour in this figure legend, the reader is referred to the Web version of this article.)



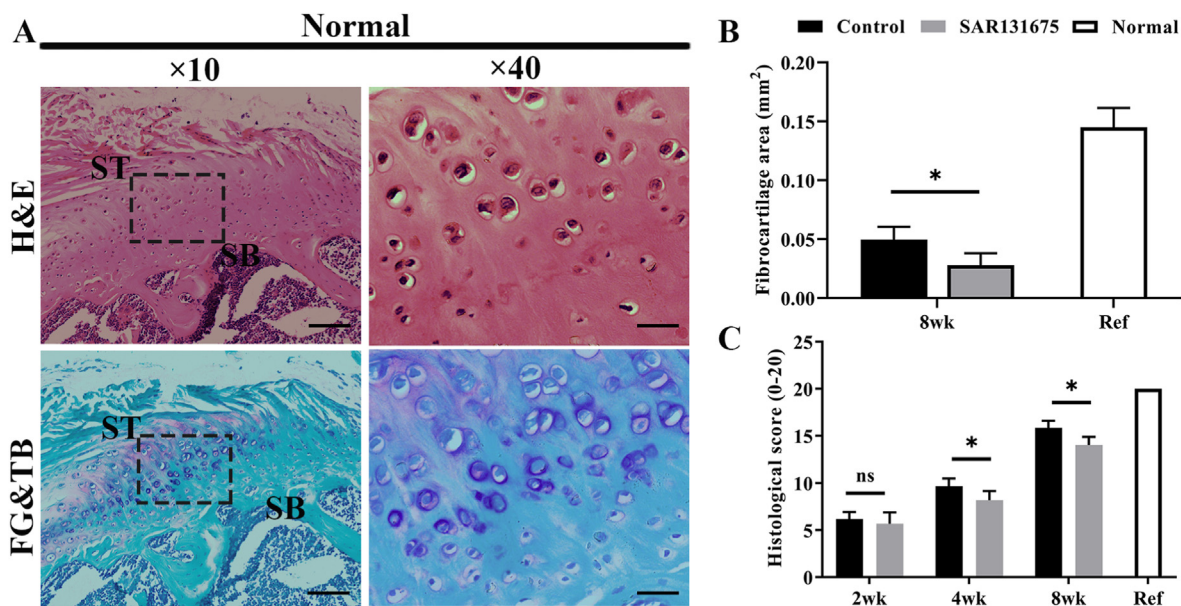


**Figure 8.** Inhibition of lymphangiogenesis at the site of injury reduces RC insertion fibrocartilage area and histological score (A) Representative histologic images of normal SST entheses. Scale bars indicate 200  $\mu\text{m}$  for the overall picture and 50  $\mu\text{m}$  for the local magnified area. H&E, hematoxylin and eosin; FG&TB, fast green and toluidine blue. (B) Quantitative analysis of the fibrocartilage area for all groups.  $n = 6$  for each group. (C) Quantitative analysis of the modified RC insertion maturity scores for all groups.  $n = 6$  for each group.  $*P < 0.05$ . (For interpretation of the references to colour in this figure legend, the reader is referred to the Web version of this article.)

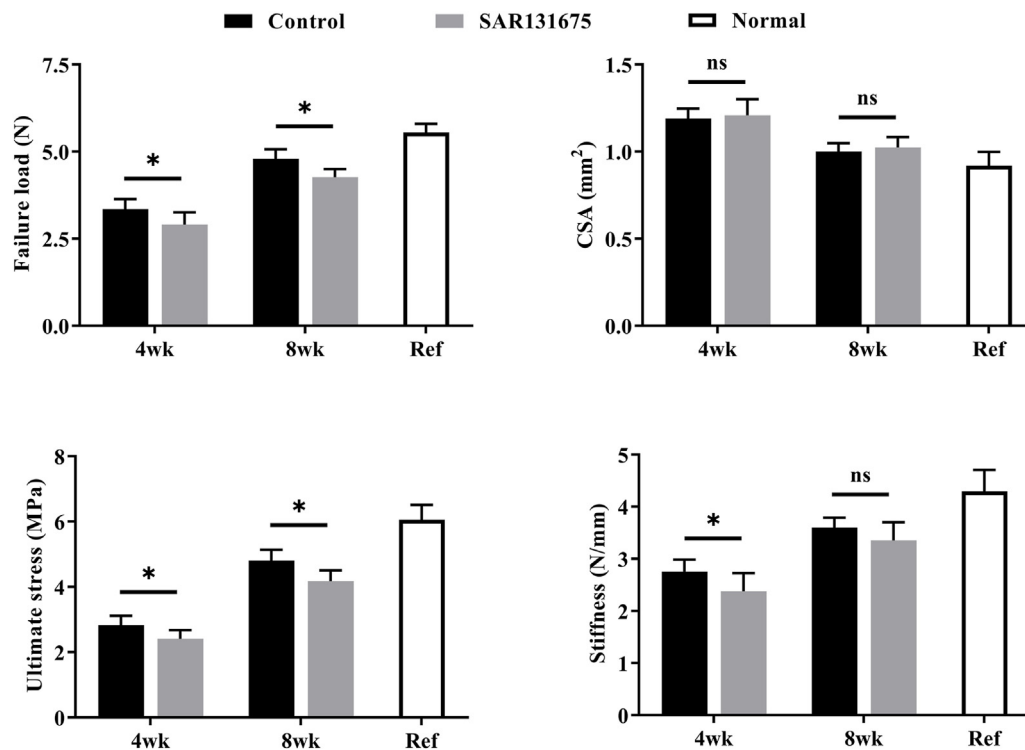


**Figure 9.** Inhibition of lymphangiogenesis at the site of injury reduces the biomechanical properties of the SS-humeral complexes. Biomechanical properties of the SS-humeral complexes.  $n = 8$  for each group.  $*P < 0.05$ .

healing, tumor formation, and tissue transplantation [28]. However, whether there exists lymphangiogenesis in the physiopathological process of RC injury repair have not been investigated yet. Specific genetic and molecular markers for lymphatic studies (LYVE-1, Podoplanin, VEGFR-3) have emerged only in recent years [29–31]. In this study, we

performed immunofluorescence co-staining of the RC insertion using lymphatic vessel specific molecular markers LYVE-1 and VEGFR-3. The results show that lymphatic vessel hyperplasia at the injury area diminished with repair time increasing. Two weeks after the procedure, the lymphatic vessels in the injured area began to proliferate; Four weeks

after surgery, the area of lymphangiogenesis gradually decreased. At postoperative week 12, the area of lymphatic proliferation was greatly reduced. It has been reported that in the early stages of inflammation, lymphangiogenic factors increase and initiate the proliferation of lymphatic endothelial cells. At the peak of inflammation, a network of lymphatic vessels begins to form. As the inflammation subsided, the area of the proliferating lymphatic vessels gradually decreased [32–34]. Lu H et al. found that during the healing process of the rabbit bone–tendon junction, two weeks after the operation was the initial period of inflammation, and the expression of pro-inflammatory cytokines decreased from the beginning 4 weeks after the operation [11]. Thankam FG et al. found in a SST injury model that inflammatory pathways started to activate in the first 2 weeks after surgery and declined after 3–4 weeks [35]. The changes in the spatiotemporal distribution of lymphatic vessels in the insertion injury area that we observed might be related to the aseptic inflammatory process that occurs after RC injury. It is well known that the lymphatic vasculature plays a regulatory role in inflammatory stage and affects tissue healing [14–17]. Based on these findings, it was reasonable to speculate that lymphangiogenesis may play an active role in RC injury healing. Interestingly, we found that the increase of lymphatic vessels remained after the RC injury was repaired (Fig. 2). Currently, there is no explanation as to why these lymphatic vessels do not disappear as inflammation decreases. One hypothesis is that the remaining lymphatic vessels have a memory function to respond rapidly to re-emerging inflammation [36].

Prior studies have indicated that the lymphatic vascular system proliferates after tissue injury, suggesting an active and possibly necessary role in tissue repair [14,16]. The damage of lymphatic vessels led to the impairment of lymphatic transport capacity, resulting in the stagnation of protein and water in the stroma, leading to tissue fibrosis and impaired immune response, thus affecting tissue repair. Guo, R et al. found that inhibition of lymphangiogenesis in a chronic arthritis model exacerbated joint synovitis, bone erosion, and cartilage loss [16]. Wang W et al. confirmed that blocking lymphatic function increased articular cartilage damage in an acute traumatic arthritis model [19]. A central question raised by the current study was whether lymphangiogenesis in RC injury site is beneficial or detrimental to its healing outcome. We utilized SAR to inhibit the lymphangiogenesis and found the drainage function of the SST was significantly weakened. Subsequently, we evaluated the healing of the two groups of RC insertion. At 4 and 8 weeks after healing, inhibition of lymphatic growth could inhibit bone growth at the interface, with decreased BV/TV, Tb.N and reduced bone staining area in H&E staining. Meanwhile, FG&TB staining showed that the area of fibrocartilage in the SAR group was significantly smaller than that in the control group. In the biomechanical test, the failure load and ultimate strength of the SAR group were significantly lower than those of the control group. This indicated that inhibition of lymphatic growth in the injured area impeded RC insertion healing. Thankam FG et al. found that upregulation of inflammatory cytokines and increased oxidative stress in a SST injury model were closely related to tendon injury pathology that impedes the healing response [35]. Viganò M et al. found that the inflammatory response following RC injury delayed the repair and healing process [37]. The possible reason was that the inhibition of lymphatic growth reduced the drainage function of tendon, aggravates local inflammation and destroyed microenvironmental homeostasis. Taken together, adequate lymphatic drainage can promote tendon insertion healing, and manipulation of the lymphatic system may be a new treatment for RC injury.

There are certain limitations in this study, firstly, although this model has been widely used to study RC injury healing mechanisms and methods to enhance healing. There are still differences between mice and humans in terms of anatomy and healing abilities. Secondly, mice are small and although tendons are load-bearing, they do not bear loads in the same way as larger animal models. In addition, this is an acute injury model while RC injuries in humans may be chronic. The findings in this mouse model may not be directly applicable to humans. Thirdly, we

observed a decrease in drainage function after lymphatic inhibition in the area of insertion injury, and there was no direct evidence that the poor healing of the RC insertion was due to the reduced drainage capacity of the tendon.

## Conclusion

We found that lymphangiogenesis was significantly increased at the insertion point injury in RC injury model mice. The inhibition of lymphatic formation at the injury site was detrimental to the healing of the tendon interface, which may be related to the reduced drainage capacity of the tendon. Together, lymphangiogenesis plays a positive role in RC healing, and targeting the lymphatic drainage at healing site may be a new therapeutic approach to promote RC injury repair.

## Author contributions

X.T., T.Z. acquisition of data, development of methodology, analysis of data, interpretation of data, drafting the manuscript. S.L., Y.C., Y.X. and C.D.: assisted in the experiments and preparation of the manuscript. H.L. and J.H.: study design, project administration. T.Z.: paper revision, method advice. All authors read and approved the final manuscript.

## Funding

This work was supported by the National Natural Science Foundation of China (No. 81730068), and the Science and Technology Major Project of Changsha (No. kh2102015).

## Declaration of Competing interest

The authors declare that they have no known competing financial interests or personal relationships that could have appeared to influence the work reported in this paper.

## Acknowledgements

The authors would like to thank professor Hui Xie and other staff from Movement

## Appendix A. Supplementary data

Supplementary data to this article can be found online at <https://doi.org/10.1016/j.jot.2022.09.014>.

## References

- [1] Sugaya H, Maeda K, Matsuki K, Moriishi J. Repair integrity and functional outcome after arthroscopic double-row rotator cuff repair. A prospective outcome study. *J Bone Joint Surg Am* 2007;89(5):953–60.
- [2] Al-Hakim W, Noorani A, Lambert S. Assessment and treatment strategies for rotator cuff tears. *Shoulder Elbow* 2015;7(2):76–84.
- [3] Klouche S, Lefevre N, Herman S, Gerometta A, Bohu Y. Return to sport after rotator cuff tear repair: a systematic review and meta-analysis. *Am J Sports Med* 2016;44(7):1877–87.
- [4] Sears BW, Choo A, Yu A, Greis A, Lazarus M. Clinical outcomes in patients undergoing revision rotator cuff repair with extracellular matrix augmentation. *Orthopedics* 2015;38(4):e292–6.
- [5] Bjornsson HC, Norlin R, Johansson K, Adolffson LE. The influence of age, delay of repair, and tendon involvement in acute rotator cuff tears: structural and clinical outcomes after repair of 42 shoulders. *Acta Orthop* 2011;82(2):187–92.
- [6] Lu H, Chen C, Qu J, Chen H, Chen Y, Zheng C, et al. Initiation timing of low-intensity pulsed ultrasound stimulation for tendon-bone healing in a rabbit model. *Am J Sports Med* 2016;44(10):2706–15.
- [7] Benjamin M, McGonagle D. Enteses: tendon and ligament attachment sites. *Scand J Med Sci Sports* 2009;19(4):520–7.
- [8] Benjamin M, Kumai T, Milz S, Boszczyk BM, Boszczyk AA, Ralphs JR. The skeletal attachment of tendons–tendon “enteses”. *Comp Biochem Physiol Mol Integr Physiol* 2002;133(4):931–45.
- [9] Derwin KA, Galatz LM, Ratcliffe A, Thomopoulos S. Entesis repair: challenges and opportunities for effective tendon-to-bone healing. *J Bone Joint Surg Am* 2018;100(16):e109.



- [10] Bianco ST, Moser HL, Galatz LM, Huang AH. Biologics and stem cell-based therapies for rotator cuff repair. *Ann N Y Acad Sci* 2019;1442(1):35–47.
- [11] Lu H, Qin L, Cheung W, Lee K, Wong W, Leung K. Low-intensity pulsed ultrasound accelerated bone-tendon junction healing through regulation of vascular endothelial growth factor expression and cartilage formation. *Ultrasound Med Biol* 2008;34(8):1248–60.
- [12] Wong MW, Qin L, Lee KM, Tai KO, Chong WS, Leung KS, et al. Healing of bone-tendon junction in a bone trough: a goat partial patellectomy model. *Clin Orthop Relat Res* 2003;413:291–302.
- [13] Vaahhtomeri K, Karaman S, Makinen T, Alitalo K. Lymphangiogenesis guidance by paracrine and pericellular factors. *Genes Dev* 2017;31(16):1615–34.
- [14] Huggenberger R, Siddiqui SS, Brander D, Ullmann S, Zimmermann K, Antsiferova M, et al. An important role of lymphatic vessel activation in limiting acute inflammation. *Blood* 2011;117(17):4667–78.
- [15] D'Alessio S, Correale C, Tacconi C, Gandelli A, Pietrogrande G, Vetrano S, et al. VEGF-C-dependent stimulation of lymphatic function ameliorates experimental inflammatory bowel disease. *J Clin Invest* 2014;124(9):3863–78.
- [16] Guo R, Zhou Q, Proulx ST, Wood R, Ji RC, Ritchlin CT, et al. Inhibition of lymphangiogenesis and lymphatic drainage via vascular endothelial growth factor receptor 3 blockade increases the severity of inflammation in a mouse model of chronic inflammatory arthritis. *Arthritis Rheum* 2009;60(9):2666–76.
- [17] Klotz L, Norman S, Vieira JM, Masters M, Rohling M, Dube KN, et al. Cardiac lymphatics are heterogeneous in origin and respond to injury. *Nature* 2015;522(7554):62–7.
- [18] Aebischer D, Iolyeva M, Halin C. The inflammatory response of lymphatic endothelium. *Angiogenesis* 2014;17(2):383–93.
- [19] Wang W, Lin X, Xu H, Sun W, Bouta EM, Zuscik MJ, et al. Attenuated joint tissue damage associated with improved synovial lymphatic function following treatment with bortezomib in a mouse model of experimental posttraumatic osteoarthritis. *Arthritis Rheumatol* 2019;71(2):244–57.
- [20] Dieterich LC, Seidel CD, Detmar M. Lymphatic vessels: new targets for the treatment of inflammatory diseases. *Angiogenesis* 2014;17(2):359–71.
- [21] Normen C, Tammela T, Petrova TV, Alitalo K. Biological basis of therapeutic lymphangiogenesis. *Circulation* 2011;123(12):1335–51.
- [22] Nihei M, Okazaki T, Ebihara S, Kobayashi M, Niu K, Gui P, et al. Chronic inflammation, lymphangiogenesis, and effect of an anti-VEGFR therapy in a mouse model and in human patients with aspiration pneumonia. *J Pathol* 2015;235(4):632–45.
- [23] Hwang SD, Song JH, Kim Y, Lim JH, Kim MY, Kim EN, et al. Inhibition of lymphatic proliferation by the selective VEGFR-3 inhibitor SAR131675 ameliorates diabetic nephropathy in db/db mice. *Cell Death Dis* 2019;10(3):219.
- [24] Kilkenny C, Browne WJ, Cuthill IC, Emerson M, Altman DG. Improving bioscience research reporting: the ARRIVE guidelines for reporting animal research. *PLoS Biol* 2010;8(6):e1000412.
- [25] Bell R, Taub P, Cagle P, Flatow EL, Andarawis-Puri N. Development of a mouse model of supraspinatus tendon insertion site healing. *J Orthop Res* 2015;33(1):25–32.
- [26] Chen Y, Zhang T, Wan L, Wang Z, Li S, Hu J, et al. Early treadmill running delays rotator cuff healing via Neuropeptide Y mediated inactivation of the Wnt/beta-catenin signaling. *J Orthop Translat* 2021;30:103–11.
- [27] Chillemi C, Petrozza V, Garro L, Sardella B, Diotallevi R, Ferrara A, et al. Rotator cuff re-tear or non-healing: histopathological aspects and predictive factors. *Knee Surg Sports Traumatol Arthrosc* 2011;19(9):1588–96.
- [28] Karpanen T, Alitalo K. Molecular biology and pathology of lymphangiogenesis. *Annu Rev Pathol* 2008;3:367–97.
- [29] Jackson DG. Biology of the lymphatic marker LYVE-1 and applications in research into lymphatic trafficking and lymphangiogenesis. *APMIS* 2004;112(7–8):526–38.
- [30] Cueni LN, Detmar M. New insights into the molecular control of the lymphatic vascular system and its role in disease. *J Invest Dermatol* 2006;126(10):2167–77.
- [31] Kaipainen A, Korhonen J, Mustonen T, van Hinsbergh VW, Fang GH, Dumont D, et al. Expression of the fms-like tyrosine kinase 4 gene becomes restricted to lymphatic endothelium during development. *Proc Natl Acad Sci U S A* 1995;92(8):3566–70.
- [32] Kataru RP, Jung K, Jang C, Yang H, Schwendener RA, Baik JE, et al. Critical role of CD11b+ macrophages and VEGF in inflammatory lymphangiogenesis, antigen clearance, and inflammation resolution. *Blood* 2009;113(22):5650–9.
- [33] Kataru RP, Kim H, Jang C, Choi DK, Koh BI, Kim M, et al. T lymphocytes negatively regulate lymph node lymphatic vessel formation. *Immunity* 2011;34(1):96–107.
- [34] Mumprecht V, Roudnicky F, Detmar M. Inflammation-induced lymph node lymphangiogenesis is reversible. *Am J Pathol* 2012;180(3):874–9.
- [35] Thankam FG, Roesch ZK, Dilisio MF, Radwan MM, Kovilam A, Gross RM, et al. Association of inflammatory responses and ECM disorganization with HMGB1 upregulation and NLRP3 inflammasome activation in the injured rotator cuff tendon. *Sci Rep* 2018;8(1):8918.
- [36] Kelley PM, Connor AL, Tempero RM. Lymphatic vessel memory stimulated by recurrent inflammation. *Am J Pathol* 2013;182(6):2418–28.
- [37] Vigano M, Lugano G, Orfei CP, Menon A, Ragni E, Colombini A, et al. Tendon cells derived from the long head of the biceps and the supraspinatus tendons of patients affected by rotator cuff tears show different expression of inflammatory markers. *Connect Tissue Res* 2021;62(5):570–9.